

Ultraviolet-Bright, High-Redshift ULIRGS

James W. Colbert¹, Harry Teplitz¹, Paul Francis², Povilas Palunas³, Gerard M. Williger^{4,5},
Bruce Woodgate⁶

ABSTRACT

We present *Spitzer* Space Telescope observations of the $z=2.38$ Ly α -emitter over-density associated with galaxy cluster J2143-4423, the largest known structure (110 Mpc) above $z = 2$. We imaged 22 of the 37 known Ly α -emitters within the filament-like structure, using the MIPS 24 μ m band. We detected 6 of the Ly α -emitters, including 3 of the 4 clouds of extended (>50 kpc) Ly α emission, also known as Ly α Blobs. Conversion from rest-wavelength 7 μ m to total far-infrared luminosity using locally derived correlations suggests all the detected sources are in the class of ULIRGs, with some reaching Hyper-LIRG energies. Ly α blobs frequently show evidence for interaction, either in *HST* imaging, or the proximity of multiple MIPS sources within the Ly α cloud. This connection suggests that interaction or even mergers may be related to the production of Ly α blobs. A connection to mergers does not in itself help explain the origin of the Ly α blobs, as most of the suggested mechanisms for creating Ly α blobs (starbursts, AGN, cooling flows) could also be associated with galaxy interactions.

Subject headings: galaxies: evolution, galaxies: high-redshift, infrared: galaxies

1. Introduction

The 110 Mpc filament mapped out by 37 Ly α -emitting objects around the $z = 2.38$ galaxy cluster J2143-4423 is the largest known structure above $z = 2$ (Palunas et al. 2004),

¹Spitzer Science Center, California Institute of Technology, Pasadena, CA 91125

²Research School of Astronomy and Astrophysics, The Australian National University, Canberra, ACT 0200, Australia

³McDonald Observatory, University of Texas, Austin, TX 78712

⁴Dept. of Physics & Astronomy, University of Louisville, Louisville, KY 40292

⁵Dept. of Physics & Astronomy, John Hopkins University, Baltimore, MD 21218

⁶NASA Goddard Space Flight Center, Greenbelt, MD 20771

comparable in size to some of the largest structures seen in the local Universe (i.e. the Great Wall, Geller & Huchra 1989). Initially identified from narrow-band imaging tuned to Ly α at $z=2.38$, it has since been spectroscopically confirmed (Francis et al. 2004; Francis & Williger 2004). In addition to its compact Ly α -emitters, this high-redshift “Filament” is also home to four extended Ly α -emitting clouds, known more commonly as Lyman α blobs.

The Ly α blob is a relatively new class of objects found among high-redshift galaxy over-densities (Steidel et al. 2000; Keel et al. 1999; Palunas et al. 2004). While similar in extent (~ 100 kpc) and Ly α flux ($\sim 10^{44}$ ergs s $^{-1}$) to high-redshift radio galaxies, blobs are radio quiet and are therefore unlikely to arise from interaction with jets. Current surveys have reported the discovery of roughly 10 of these giant Ly α blobs, but they are not isolated high redshift oddities. Matsuda et al. (2004) have demonstrated that the blobs are part of a continuous size distribution of resolved (>16 arcsec 2) Ly α emitters, with more than 40 presently known.

One of the standing mysteries of the blobs is the source of their energy, as the measured ultraviolet flux from nearby galaxies is insufficient to produce the observed Ly α fluxes. One possibility is that the Ly α blobs are powered by supernova-driven superwinds (Ohyama & Taniguchi 2004), driving great plumes of gas into the surrounding ambient medium and producing shocks. An obscured AGN is another model, with the exciting ultraviolet illumination escaping along different lines of sight (i.e., Basu-Zych & Scharf 2004). Cooling flows have also been suggested (Fardal et al. 2001; Francis et al. 2001) as a possible power source.

There is growing evidence that Ly α blobs mark regions of extreme infrared luminosity. Submillimeter flux has been detected in two of the giant Ly α blobs, SMM J221726+0013 (Chapman et al. 2001) and SMM J17142+5016 (Smail et al. 2003). The submm source SMM J02399-0136 is also likely surrounded by a Ly α blob halo, as its Ly α emission covered most of a 15'' slit (Ivison et al. 1998). Most recently, Geach et al. (2005) has detected submm flux from four of the smaller (< 55 square arcsec) and less luminous ($< 2 \times 10^{43}$ L $_{\odot}$) Ly α blobs from Matsuda et al. (2004): LAB5, LAB10, LAB14 & LAB18. Also, Dey et al. (2005) has discovered a single Ly α blob (SST24 J1434110+331733) in the NOAO Deep Wide-Field Survey with strong 24 μ m flux (0.86 mJy).

In this paper we discuss the *Spitzer* 24 μ m observations of these $z=2.38$ Ly α -emitters, both compact sources and blobs. We estimate the total far-infrared luminosity for all detections and discuss the possibility of a connection between mergers and Ly α blobs. We assume an $\Omega_M=0.3$, $\Omega_\Lambda=0.7$ universe with $H_0=70$ km s $^{-1}$ Mpc $^{-1}$.

2. Observations

Our data were obtained using Multiband Imaging Photometer for Spitzer (MIPS; Rieke et al. 2004) in $24\mu\text{m}$ photometry mode. The field was observed on October 13 and 14 and November 4 and 5, 2004. The primary observation was a 3×5 raster map, covering approximately 15×25 arcminutes of the filament structure, centered at $21^{\text{h}}42^{\text{m}}38.0^{\text{s}}$, $-44^{\circ}26'30''$. The total integration time per pixel is 1818 seconds. In addition we observed one small side field (5×5 arcmin) with a single known $\text{Ly}\alpha$ -emitter (at $21^{\text{h}}42^{\text{m}}56.3^{\text{s}}$, $-44^{\circ}37'57''$) for 666 seconds. The data were initially reduced by the standard *Spitzer* pipeline¹. We then produced sky frames for each data frame from the median of the 100 nearest (in time) data frames.

We assembled the final mosaic of the MIPS $24\mu\text{m}$ image using the MOPEX package available from the *Spitzer* Science Center. The final drizzled pixel scale is $1.23''$ per pixel. For source extraction, we applied the APEX source extraction package available within MOPEX. APEX requires an input Point Response Function (PRF), which we created from the 40 brightest objects extracted from the final image. Our final APEX source extraction detected 3010 objects down to roughly $50\mu\text{Jy}$. The full dataset will be discussed in a future paper.

The $5\text{-}\sigma$ detection limit, as measured within a $7.5''$ aperture, is $58\mu\text{Jy}$ over most of the image, but can be as high as $180\mu\text{Jy}$ at the edges. None of the $\text{Ly}\alpha$ -emitters for which APEX failed to find MIPS sources had aperture fluxes greater than these $3\text{-}\sigma$ upper limits. A list of all extracted MIPS sources associated with $\text{Ly}\alpha$ -emitters is presented in Table 1. A brief note on the naming conventions: The first three $\text{Ly}\alpha$ -emitters were found by Francis et al. (1996) and named B1, B2, & B3. Further study by Francis et al. (1997) demonstrated that the B3 source was not real, but they also found another source, which they labeled B4. Palunas et al. (2004) found 34 additional $\text{Ly}\alpha$ -emitters in the field and so, rather than label each one, only gave B# designations to the three new $\text{Ly}\alpha$ blobs: B5, B6, & B7. We continue the B# naming convention, adding sources B8 and B9.

3. MIPS Detections of $\text{Ly}\alpha$ Sources

Six out of 22 ($\sim 30\%$) of the $\text{Ly}\alpha$ -emitters within the filament are associated with MIPS $24\mu\text{m}$ sources (Figure 1), including three of the four resolved (>50 kpc) $\text{Ly}\alpha$ blobs. This blob association rate is much higher than that for unresolved $\text{Ly}\alpha$ -emitters (Only 3 of 18). We determined a MIPS source to be associated if it lies within one MIPS FWHM ($5.9''$) of

¹<http://ssc.spitzer.caltech.edu>

the position of the Ly α -emitter. In four cases the coordinates for the MIPS and Ly α sources agree to less than an arcsecond, while the remaining two are separated by 2.7 (Blob B7) and 4.1'' (source B9). We checked the MIPS field astrometry against that of the optical data by comparing object centroids for all detected MIPS sources against those found in I-band. After correction for a 0.3'' offset, we found that the positions of the objects agree with a standard deviation of 1.5''.

The density of MIPS sources in the central portion of the field is $\sim 4.5 \text{ arcmin}^{-2}$, making the odds of a chance superposition of a random MIPS source $< 0.4\%$ for those within an arcsecond, $< 2.9\%$ for within 2.7'', and $< 6.6\%$ for within 4.1''. However, all the detected Ly α -emitter counterparts have fluxes greater than 120 μJy , well above the detection limits and with a consequently lower surface density. Accounting for source brightness decreases the probability of chance superposition below 0.3% for all sources except for source B9, which has a 3.3% chance that its associated MIPS source (4.1'' away) is mere coincidence. For comparison, the Dey et al. (2005) MIPS source lies 2.5'' from the center of its associated Ly α blob.

We do not detect 16 of the 22 Ly α -emitters in the MIPS image. Six of these sources lie in regions of higher noise, where the 5σ detection limits range from 100-180 μJy . The remaining ten Ly α -emitters are in the central regions of the image, with detection limits of $< 60 \mu\text{Jy}$. The lack of faint MIPS counterparts is unlikely to be a result of error in object positions, as we examine a radius nearly 4 times the typical 1σ offset found from matching the MIPS and optical data. The absence of detections between 60 and 120 μJy indicates there is not a rapid climb in numbers with decreasing $24\mu\text{m}$ flux for Ly α -emitters over this range, although the number of objects considered is small.

Two of the Ly α blobs, B6 and B7, appear to have additional MIPS sources associated with them. The B6 Ly α blob extends over 25'', or over 200 kpc at $z=2.38$, and contains more than one knot or concentration. The brightest Ly α knot is the central one and it is associated with a bright MIPS source, but the southern knot (not to be confused with the large diffuse area to the southeast) also has a MIPS source of almost identical brightness. There is also an area of more diffuse Ly α emission to the north which also appears to be associated with a bright MIPS source. Each source is separated by approximately 9.5'' from the central source, creating a potential triple system. The northern source should probably be treated with some caution, as it not only lacks any clear Ly α concentration, but there is also a relatively bright galaxy visible at that location in the B-band image (B=22.5), which is unlikely to be at high redshift.

The center of the B7 Ly α blob actually lies between two sources. We have associated it with the brighter, closer MIPS source 2.7'' (~ 20 kpc) to its southeast, but a second source

lies $5.9''$ (~ 45 kpc) to the northwest. While there is a $\sim 10\%$ chance the second object could be chance association, the location of the $\text{Ly}\alpha$ blob immediately between the two MIPS sources suggests a possible physical connection.

4. Ultraviolet-Bright ULIRGs

The detected $24\mu\text{m}$ flux densities range from 0.1 to 0.6 mJy, which at $z=2.38$ corresponds to roughly 2×10^{11} to $10^{12} L_{\odot}$ in rest frame $7\mu\text{m } \nu F_{\nu}$. To convert from the mid-infrared to total bolometric luminosity (L_{bol}), we use the relationship from Chary & Elbaz (2001), hereafter CE01, calibrated by examining galaxies measured with both ISO and IRAS:

$$L_{\text{IR}} = 4.37_{-2.13}^{+2.35} \times 10^{-6} \times L_{6.7\mu\text{m}}^{1.62} \quad (1)$$

In an effort to avoid over-estimation of L_{IR} , the mid-infrared conversion used throughout this paper assumes the low end of the 1σ envelope, producing total luminosities roughly a factor of 2 lower than a direct application of the formula. Even this conservative mid-IR conversion puts all the sources in the class of ultra luminous infrared galaxies (ULIRGs; $> 10^{12} L_{\odot}$), with many achieving Hyper-LIRG ($> 10^{13} L_{\odot}$) status (see Figure 2). It should be noted, however, that the CE01 relation is based on nearby starburst-dominated galaxies and it is possible it may not hold at high redshift or for the most extreme starbursts, if their spectral energy distributions are significantly different.

The L_{bol} of most ULIRGs in the nearby universe comes from a combination of strong star formation and AGN activity (see Sanders & Mirabel 1996, for review). The majority are dominated by the stellar component, seen both in the far-infrared to radio relation (Yun, Reddy, & Condon 2001) and their strong PAH to continuum ratios (Lutz et al. 1998). However, this changes as the luminosity approaches that of the Hyper-LIRG ($\text{LIR} > 10^{13} L_{\odot}$); AGNs typically dominate above $\sim 10^{12.5} L_{\odot}$ (Tran et al. 2001). It is presently unknown how this trend will continue out to higher redshifts, where high-mass mergers, like those predicted to build giant ellipticals, could be producing energies on the scale of a Hyper-LIRG through star formation (Dopita et al. 2005). PAHs are already being found in high-redshift infrared sources (Houck et al. 2005; Yan et al. 2005). If these MIPS sources are AGN-dominated, one would expect $F_{\nu} \propto \nu^{-1}$, which would still place all the detected sources in the class of ULIRGs.

If we combine the $24\mu\text{m}$ detections from this study and from Dey et al. (2005) with the submm detections of $\text{Ly}\alpha$ blobs (Chapman et al. 2001; Smail et al. 2003; Geach et al. 2005), there are now at least 10 known high redshift ULIRGs surrounded by $\text{Ly}\alpha$ halos. We plot

$\text{Ly}\alpha$ luminosity versus L_{bol} for all the identified $\text{Ly}\alpha$ blobs with infrared or submm detections in Figure 3. SMM J02399-0136 (Ivison et al. 1998) is excluded as its total $\text{Ly}\alpha$ flux is not precisely known. We use the published L_{bol} values for all submm sources, but derive the total L_{bol} for the Dey et al. (2005) $24\mu\text{m}$ source using the CE01 relation to better compare with our results.

Applying a similar analysis, Geach et al. (2005) found a weak $\text{Ly}\alpha/\text{IR}$ relation for submm-detected $\text{Ly}\alpha$ blobs with a typical $L_{\text{Ly}\alpha}/L_{\text{bol}}$ ratio just under 0.1%. Including our $24\mu\text{m}$ -detected $\text{Ly}\alpha$ blobs, which are brighter in $\text{Ly}\alpha$ than most of the Geach et al. (2005) objects, we continue to see the same weak trend, with a $L_{\text{Ly}\alpha}/L_{\text{bol}}$ efficiency of 0.05-0.2%. Neither the detection of X-rays (SMM J17142+5016 & LAB18) nor CIV emission (B1, SMM J17142+5016, & SST24 J1434110+331733), both strong indicators of AGN activity, has any clear effect on this trend. There is one significant outlier, the B5 blob, which falls at least a factor of 30 away from this proposed relation. While this relation is still tentative, it suggests a direct causal connection between the ULIRG infrared luminosity and the $\text{Ly}\alpha$ blobs.

5. $\text{Ly}\alpha$ Blob Merger Connection?

The high rate of MIPS detection for the $\text{Ly}\alpha$ blobs (3 out of 4) demonstrates that these ultraviolet sources are locations of tremendous infrared energy. Two of the $\text{Ly}\alpha$ blobs (B6 & B7) are associated with multiple MIPS sources, suggesting possible interaction or even merger. These separations between possible ULIRG component galaxies are large (60-70 kpc) compared to the typical low-redshift ULIRG, which have a median separation ~ 2 kpc (Murphy et al. 1996). However, interacting ULIRGs with wide separations on the scale of 50 kpc do exist (Kim et al. 2002), and seem to occur when at least one the interacting galaxies is highly gas-rich (Dinh-V-Trung et al. 2001).

Previous high resolution *HST* imaging also indicates a possible $\text{Ly}\alpha$ blob connection to merging galaxies. For instance, NICMOS imaging of blob B1 shows a pair of compact, red galaxies with a projected separation of less than 7 kpc (Francis et al. 2001). Only three other $\text{Ly}\alpha$ blobs have been imaged with *HST*: the blobs in the field of 53W002, one of which shows a second nearby galaxy (Keel et al. 1999), and blob SSA22a-C11 (Steidel et al. 2000) which STIS imaging shows to be composed of several likely interacting components (Chapman et al. 2004). Dey et al. (2005) also find multiple components within their blob, visible in their ground-based, optical imaging.

In the local universe, the most energetic mergers are associated with the ULIRGs, with roughly 90% of ULIRGs clearly interacting (Bushouse et al. 2002; Farrah et al. 2001). The

majority of local ULIRG mergers are between two low mass ($0.3\text{--}0.5 L^*$) galaxies (Colina et al. 2001), but major mergers of high-mass galaxies, like those predicted to build giant ellipticals, must be occurring at higher redshift (i.e., Conselice 2005). If merger-induced star formation is the source of the majority of the infrared flux in these objects, it implies star formation rates of 1000s of $M_\odot \text{ yr}^{-1}$, like those suggested for some sub-mm sources (Chapman et al. 2003; Geach et al. 2005). Such massive SFRs would be capable of generating the supernova kinetic energy needed to drive a superwind and power the $\text{Ly}\alpha$ blobs. If supernovas deposit roughly 10^{49} ergs per solar mass of stars into the surrounding medium (i.e., Bower et al. 2001), a star formation rate of $1000 M_\odot \text{ yr}^{-1}$ will easily match the $\sim 10^{51}$ ergs yr^{-1} emitted by the blobs, even at a low efficiency.

Mergers could also help drive gas inwards into a supermassive black hole, making AGN another viable infrared energy source, with escaping ultraviolet radiation driving the $\text{Ly}\alpha$ blobs. Dey et al. (2005) found that their $24\mu\text{m}$ -detected blob is better fit by an AGN spectral energy distribution than that of a star forming galaxy, but longer rest-wavelengths or a mid-IR spectrum are required for a definitive determination. There is one clearly starbursting galaxy at the northern end of their $\text{Ly}\alpha$ nebula.

Cooling flows also remain a possibility, as it might be common to find multiple galaxies merging at the center of such a large inward flow of gas. It does become a less favored model, however, as the energy from the cooling gas is no longer required to power the $\text{Ly}\alpha$ blobs. The ULIRGs would appear to have more than enough energy in their budget to do so on their own.

This work is based on observations made with the *Spitzer* Space Telescope, which is operated by the Jet Propulsion Laboratory, California Institute of Technology, under NASA contract 1407. We wish to acknowledge financial support from the *Spitzer* grant GO-3699.

REFERENCES

- Basu-Zych, A. & Scharf, C. 2004, *ApJL*, 615, L85
- Bower, R. G., Benson, A. J., Lacey, C. G., Baugh, C. M., Cole, S., & Frenk, C. S. 2001, *MNRAS*, 325, 497
- Bushouse, H. A., et al. 2002, *ApJS*, 138, 1
- Chapman, S. C., et al. 2004, *ApJ*, 606, 85
- Chapman, S. C., Windhorst, R., Odewahn, S., Yan, H., & Conselice, C. 2003, *ApJ*, 599, 92

- Chapman, S. C., Lewis, G., Scott, D., Richards, E., Borys, C., Steidel, C., Adelberger, K., & Shapley, A. 2001, *ApJ*, 548, L17
- Chary, R., & Elbaz, D. 2001, *ApJ*, 556, 562
- Colina, L., et al. 2001, *ApJ*, 563, 546
- Conselice, C. J. 2005, *ApJ*, accepted, astro-ph/0405001
- Dey, A., et al. 2005, *ApJ*, accepted, astro-ph/0503632
- Dinh-V-Trung et al. 2001, *ApJ*, 556, 141
- Dopita, M. A., et al. 2005, *ApJ*, 619, 755
- Fardal, M. A., Katz, N., Gardner, J. P., Hernquist, L., Weinberg, D. H., & Davé, R. 2001, *ApJ*, 562, 605
- Farrah, D., et al. 2001, *MNRAS*, 326, 1333
- Francis, P. J., Palunas, P., Teplitz, H. I., Williger, G. M., & Woodgate, B. E. 2004, *ApJ*, 614, 75
- Francis, P. J., & Williger, G. M. 2004, *ApJL*, 602, L77
- Francis, P. J., et al. 2001, *ApJ*, 554, 1001
- Francis, P. J., Woodgate, B., & Danks, A. 1997, *ApJL*, 482, L25
- Francis, P. J., et al. 1996, *ApJ*, 457, 490
- Geach, J. E., et al. 2005, submitted to *MNRAS*, astro-ph/0508357
- Geller, M. J., & Huchra, J. P. 1989, *Science*, 246, 897
- Houck, J. R., et al. 2005, *ApJL*, 622, L105
- Iverson, R. J., Smail, I., Le Borgne, J.-F., Blain, A., Kneib, J.-P., Bezecourt, J., Kerr, T., & Davies, J. 1998, *MNRAS*, 298, 583
- Keel, W. C., et al. 1999, *AJ*, 118, 2547
- Kim, D. -C., Veilleux, S., & Sanders, D. B. 2002, *ApJS*, 143, 277
- Lutz, D., et al. 1998, *ApJL*, 505, L103

- Matsuda, Y., et al. 2004, AJ, 128, 569
- Murphy, T., et al. 1996, AJ, 111, 1025
- Ohyama, Y. & Taniguchi, Y. 2004, AJ, 127, 1313
- Palunas, P., et al. 2004, ApJ, 602, 545
- Rieke, G. H., et al. 2004, ApJS, 154, 25
- Sanders, D. & Mirabel, I. 1996, ARAA, 34, 749
- Smail, I., Ivison, R. J., Gilbank, D. G., Dunlop, J. S., Keel, W. C., Motohara, K., & Stevens, J.A. 2003, ApJ, 583, 551
- Steidel, C. C., et al. 2000, ApJ, 532, 170
- Tran, Q. D., et al. 2001, ApJ, 552, 527
- Yan, L., et al. 2005, ApJ, 628, 604
- Yun, M. S., Reddy, N. A., & Condon, J. J. 2001, ApJ, 554, 803

Table 1. Ly α Sources

RA	Dec	$\log L_{Ly\alpha}$ ergs s $^{-1}$	$24\mu\text{m } F_\nu$ μJy	νL_ν $10^{10} L_\odot$	Total FIR $10^{10} L_\odot$	Comment
21:42:27.59	-44:20:29.7	43.9	236	33.4	1000	Blob B1
21:42:32.16	-44:20:18.5	43.0	562	79.5	4300	B4
21:42:42.66	-44:30:09.4	43.8	634	89.5	5200	Blob B6
21:42:34.95	-44:27:08.8	43.5	292	41.3	1500	Blob B7; 2.7'' offset
21:43:05.84	-44:27:20.9	43.7	142	20.1	460	B8
21:43:37.33	-44:23:56.2	43.1	123	17.4	360	B9; 4.1'' offset
21:43:03.57	-44:23:44.2	43.8	< 58	< 8	< 80	Blob B5
Possible Ly α Blob Companions						
21:42:42.79	-44:30:18.2	n/a	535	76	3900	9.5'' from B6
21:42:42.49	-44:29:59.8	n/a	340	48	1900	9.5'' from B6
21:42:34.68	-44:27:01.2	n/a	172	24	620	5.9'' from B7

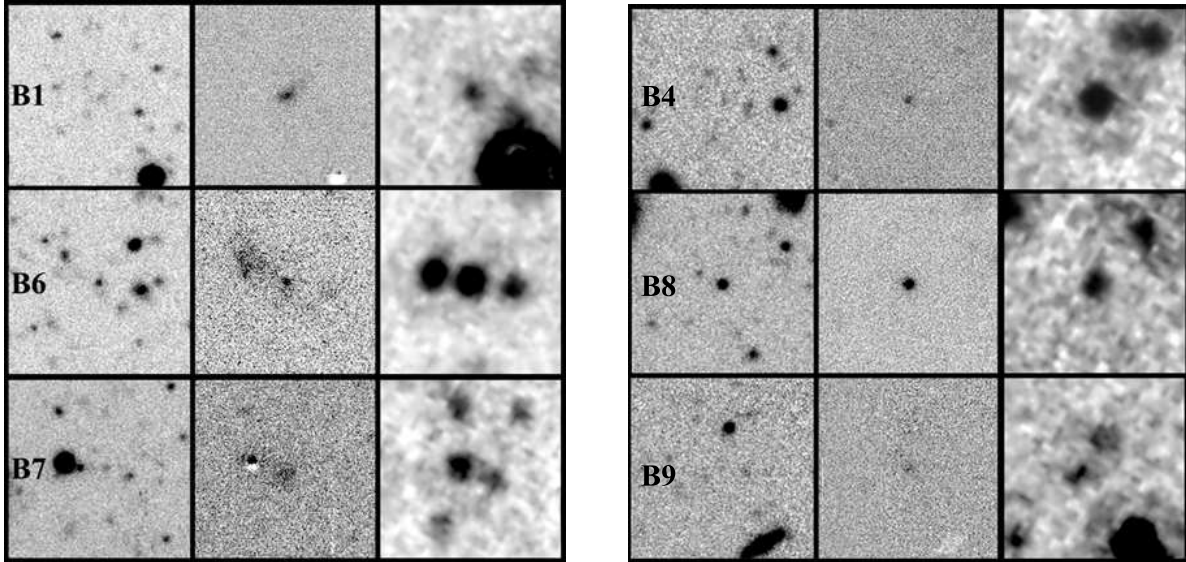


Fig. 1.— Left) Images of the $40'' \times 40''$ field around the three MIPS-detected Ly α blobs: B1, B6, & B7. From left to right the images are CTIO B-band, CTIO continuum-subtracted Ly α , and MIPS $24\mu\text{m}$. East is upwards, north to the right. One arcsecond corresponds to 8kpc at $z=2.38$. Right) Images of the $40'' \times 40''$ field around the three MIPS-detected non-extended Ly α -emitters. Format is same as left.

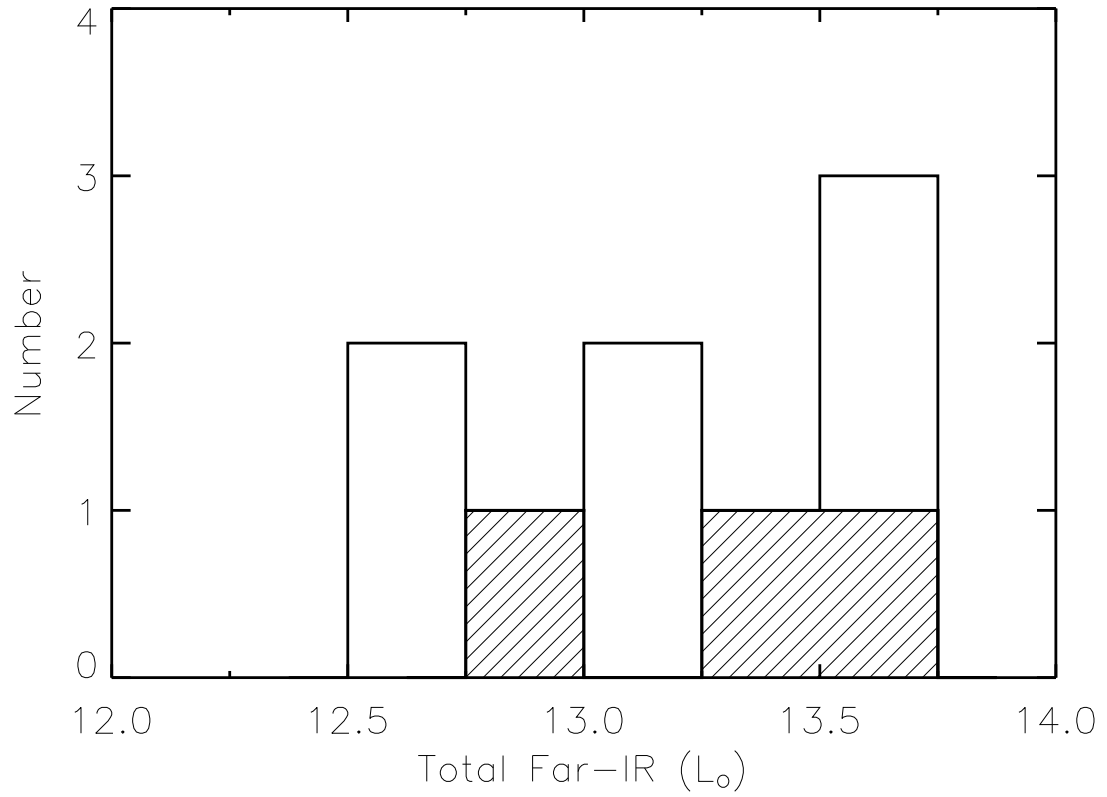


Fig. 2.— Histogram of inferred total far-infrared luminosity for MIPS sources associated with $z=2.38$ $\text{Ly}\alpha$ sources. The three sources potentially associated with the $\text{Ly}\alpha$ blobs B6 and B7 are marked with cross-hatching.

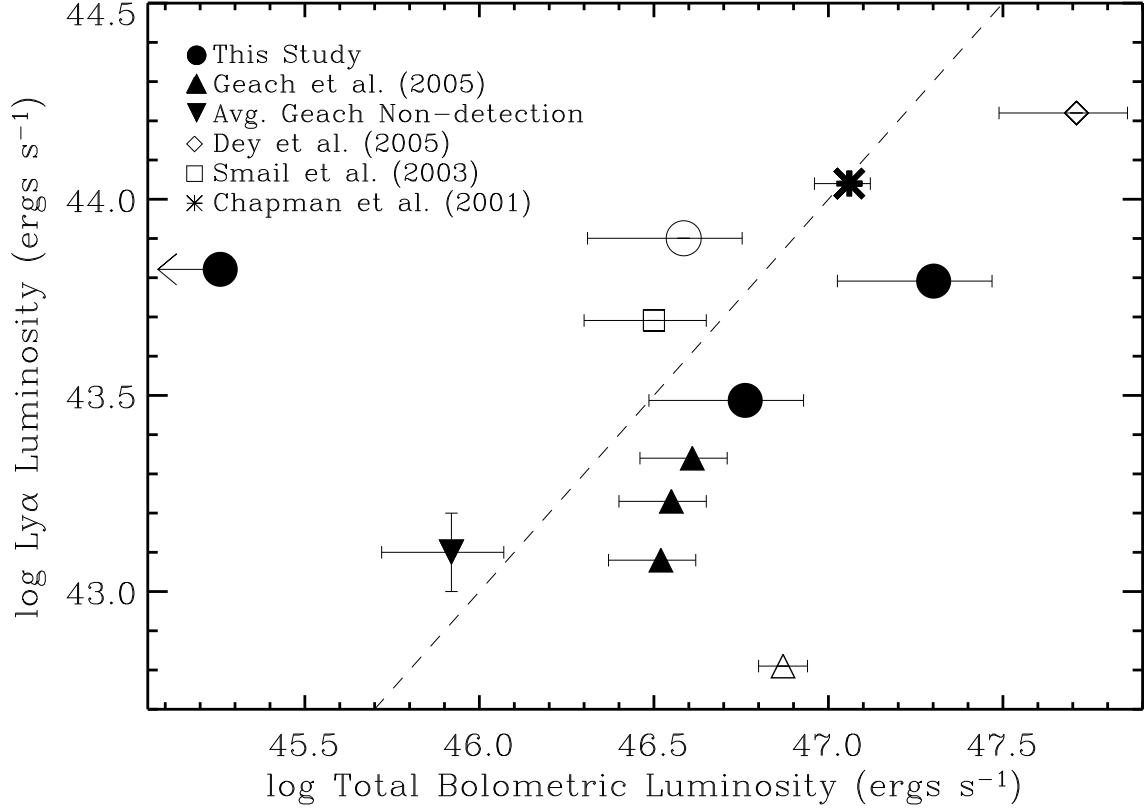


Fig. 3.— Log $L_{Ly\alpha}$ vs. log L_{bol} for high- z Ly α blob ULIRGs. The $24\mu\text{m}$ -detected blobs are the circles (This study) and the diamond (Dey et al. 2005), with error bars based on the estimated reliability of the Chary & Elbaz (2001) relation. The submm detections are the triangles (Geach et al. 2005), squares (Smail et al. 2003), and asterisks (Chapman et al. 2001). The upside-down triangle is the average of all non-detected Geach et al. blobs. Ly α blobs with evidence for AGN activity (X-rays or CIV emission) are plotted as hollow symbols. The dashed line marks where $L_{Ly\alpha}/L_{bol} = 0.001$.